

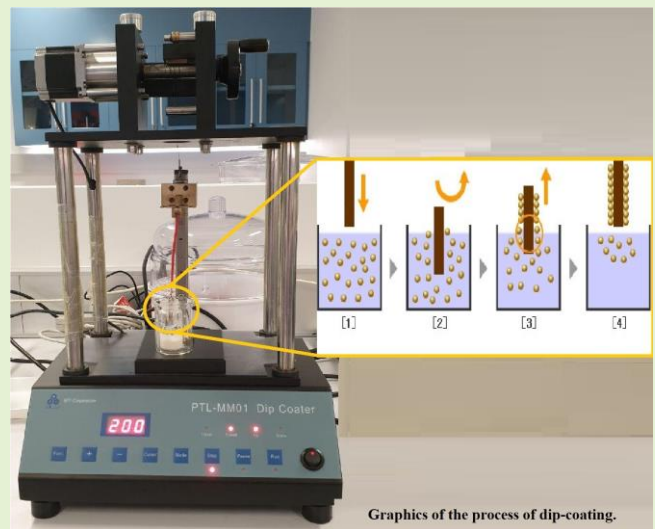
Functionality Evaluation of Micro-Electro-Mechanical-Systems Sensor for Varied Selective Functionalization Thickness to Determine Creatinine Concentration

Sumedha Nitin Prabhu, *Graduate Student Member, IEEE*
Subhas Chandra Mukhopadhyay, *Fellow, IEEE*
Rosario Morello, *Member, IEEE*

Abstract— The sensitivity and the selectivity are the most significant parameters of any sensor. In this paper, the effect of the coating (functionalization) thickness on the performance associated with the sensitivity of a Micro-Electro-Mechanical-Systems (MEMS) planar interdigital (ID) sensor is studied. The MEMS sensors are preferred due to their small size and high sensitivity. With acrylic resin and the Molecularly Imprinted Polymer (MIP), selective functionalization's over the MEMS sensor sensing area and their detection capability is successfully analysed with heat-inactivated human serum samples having varying creatinine concentration. The performance-based coated-sensor analysis has been identified. The developed MIP coated MEMS ID sensors detection limit is 50 ppm, which is three times higher than the level of creatinine in real human serum.

The MIP-coated selective MEMS sensor functionalization exhibited the highest sensitivity while measuring creatinine levels from the heat-inactivated human serum samples. The net effect of material properties, speed of withdrawal and time of dipping on the functionalization layer thickness is efficaciously investigated. This study found out that the faster speed of withdrawal would result in a thinner layer of functionalization. The functionalization layer thickness is increased with an increase in the net time of dipping. However, the findings have effectively shown that rising the sensor functionalization thickness substantially raises the saturation level.

Index Terms— Micro-Electro-Mechanical-Systems (MEMS), planar interdigital (ID) sensor, Molecularly Imprinted Polymer (MIP), creatinine.



I. INTRODUCTION

ELIMINATING the natural and synthetic contaminants from the sensing surface is one of the most critical tasks in sensing research to get precise detection of the targeted molecules. The addition of a protective layer of surface functionalization is known as the most efficient protective methodology that has been practised everywhere in controlling the natural and synthetic contaminant impact. Different studies on the functionalization layer have been undertaken in controlling the process of corrosion and improving the corrosive resistance [1], [2], for detecting natural contaminants [3] and also in avoiding biological interventions [4] - [6]. Furthermore, the protection of a sensing surface is done by functionalizing the membrane using natural and synthetic reactions where they act like a precisely selective layer. The incorporation of a specifically selective layer of functionalization raises the sensor selectivity in detecting the

target molecule. The specifically selective layer of functionalization's has been stated in the detection of various molecules including, a marker of ovarian cancer [7], presence of phthalate in beverages [8], cholesterol [9], etc.

In the presented studies, the method of dip coating with the help of the PTL-MM01 Dip Coater instrument is utilised in generating the layer of functionalization on the surface of the Micro-Electro-Mechanical-Systems (MEMS) sensor. From the list of simplified and most used techniques, including the spin coating [10], [11] as well as the spray coating [12], [13], the process of dip coating is frequently used. This technique is well-known, and we used it because of its notable features such as cost-effectiveness, reproducibility, and operational easiness. In the present work, the sensing area of the MEMS sensor is immersed inside the functionalization solution and then removed at a pre-decided speed and time of immersion. The functionalization solution uniformly coated the sensing surface area of the MEMS sensor. Post functionalization of the sensor sensing area, it gets dried up due to the natural process

of evaporation. A hard layer of functionalization gets generated over the MEMS sensing area [4], [14] - [16]. The thickness and consistency of the functionalization solution, speed of withdrawal, dipping time, the temperature of the functionalization solution, and the evaporation speed of the chemical components used while making the process of the functionalization layer characteristics of the MEMS sensor [1], [14], [17]. The graphics of the process of dip coating is displayed in the graphical abstract. In the present work, the effect of withdrawal speed and of the time of dipping during the dip coating process is assessed.

Creatinine is a toxic metabolic waste, and it is formed daily inside the body of all the vertebrates [18]. The creatinine acts as a functional biomarker in deciding the kidneys functioning [19] - [21]. Research using Molecularly Imprinted Polymer (MIP) based study has been recorded for the detection and measurement of creatinine [22], [18], [23], [24]. This work is a middle part of our previously published articles [18], [23]. In the presented work, serum creatinine samples with varying creatinine concentrations are used to estimate the performance of the MEMS sensor.

The MEMS sensor's functional sensitivity is significantly dependent on the functionalization layer thickness. Hence, in the presented study, we have examined the functionalization layer's role in detecting and measuring creatinine. We have also studied the effect of functionalization layer thickness on the performance of the MEMS planar interdigital (ID) sensor on the creatinine measurement. The acrylic functionalization and the creatinine-specific selective MIP functionalization layers are analysed for calculating the MEMS ID sensor functional performances associated with the sensitivity.

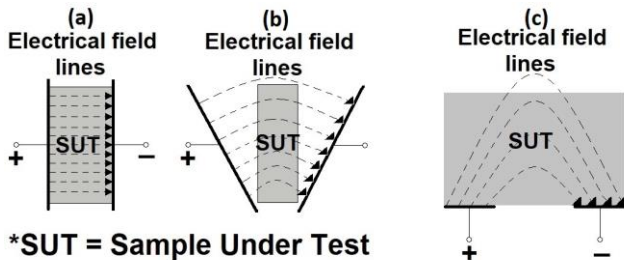


Fig. 1. Adaptation of the parallel plate design into the planar ID MEMS sensor (a) parallel plate capacitor, (b) intermediate stage and (c) ID sensor [24].

II. WORKING PRINCIPLE OF MEMS SENSOR WITH PLANAR ID ELECTRODES

Standard planar shaped ID sensors have a repetitive pattern of electrodes in a parallel plane. The electric field lines are formed with the application of an alternating current (AC) excitation signal to the ID electrodes. These field lines enter inside the sample under test (SUT) and capture the SUT-related information [25]. The planar ID sensors are coplanar-shaped parallel plate capacitor structures that adopt the same concept and give single-sided access to the SUT. The conversion into the planer-shaped structure of the parallel plate capacitor is shown in Fig. 1. The transition process alters the electrical field uniform flow to the protruding electrical

field, which in turn passes through the SUT. It produces an output that is directly proportional to the SUT properties. Whilst passing through SUT, the absolute permittivity of the penetrating electrical field changes due to the different electrochemical characteristics of the SUT. The shift in the electrical field is analysed as a functional characteristic of the sensor [20]. The alternately charged finger-alike structured design of the ID sensor is frequently repeated multiple times for raising the strength of the output signals [25].

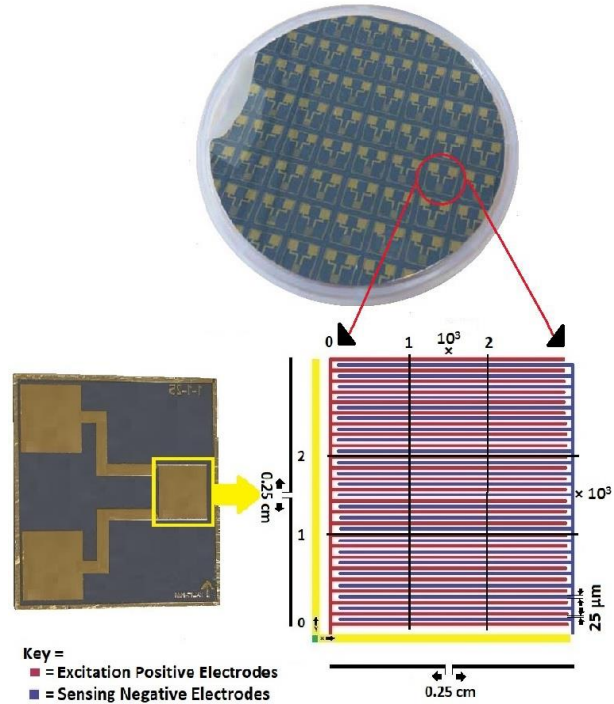


Fig. 2. A MEMS technology-based sensor fabricated using a silicon wafer and a diagrammatic representation of the individual sensing area of the MEMS sensor.

An ID sensor with an equal number of negative sensing and positive excitation electrodes has been designed and fabricated with a 1-1-25 configuration [23], [24], [26] - [28]. The critical determination during the design of an equal positive-negative electrode patterned sensor is to achieve uniformity in precise detection, to raise the sensor sensitivity, and to refine the response towards the SUT. The ID patterned sensor chips are designed on a single side of a 2-inch diameter silicon wafer with etching and photolithography techniques. Gold electrodes with an ID pattern and thickness of 500 nm have been designed by gold sputtering over the silicon wafer substrate. Total 36 units of working sensors are developed on the silicon wafer chip where every sensor has a structural design of 10 mm \times 10 mm. Fig. 2 denotes the sensing area of the developed sensor, which is 2.5 mm \times 2.5 mm [29]. A chip-sized sensor made on a silicon wafer with a 1-1-25 design configuration has been utilised to carry out the experiments. The 1-1-25 sensor included 1 sensing negative electrode between 2 excitation positive electrodes with an alternative pattern. The pitch length spacing in-between consecutive electrodes of 25 μ m is used in performing the experiments.

The electrochemical impedance spectroscopy (EIS)

technique is utilised for analysing the dielectric properties of materials. The EIS technique is found out to be the most suitable for analysing electrode kinetics of electrochemical systems having huge complexity. In the proposed methodology, excitation signals having low amplitude are necessary because of the non-linearity formed by the electron transfer process [30], [31]. This technology is broadly utilised in biomedical healthcare applications [32], [33], corrosive materials [34], and also in measuring food and beverages contamination levels [34], [35]. The EIS is defined as a reaction of an electrochemical system with an AC impulse in simplified terms. The real impedance and the imaginary impedance are the integral parts of the impedance widely utilised in reflecting the device outcome to the applied potential. The outcome obtained is in a composite system, and it is showcased using the Nyquist plotting method.

III. MATERIAL AND METHODS

A. Chemicals, Apparatus and Instruments

The creatinine powder, methacrylic acid (MAA), 2, 2-azoisobutronitrile (AIBN), divinylbenzene, acetonitrile, toluene, acetic acid, acrylic resin, acetone are used for this experiment. All these chemicals are procured from Sigma-Aldrich, Australia. All glassware is also purchased from Sigma-Aldrich, Australia. PTL-MM01 Dip Coater instrument for obtaining a functionalization layer uniformity. The high precision Hioki 3536 LCR meter instrument is used for measuring the output of the MEMS sensor. The JEOL JSM 7100F Field Emission Scanning Electron Microscope (FESEM) instrument is used for obtaining high-definition images of the MEMS sensor surface. The fabrication details of the MEMS ID sensor are described in our publication [36].

B. Surface Functionalization of the MEMS Sensor with Acrylic Resin

The acrylic resin is used to coat the planar ID sensor. The sensing surface is washed with acetone to remove any invisible surface debris or contaminations in the first step. In the second step, the acrylic resin coat is made by mixing acetone as a liquefier (1.5 mL) and acrylic resin (200 μ L) as a protective layer and adhesive agent. It is layered on the MEMS sensor sensing area as a protecting layer of functionalization and acts as an adhesive agent. The layering of acrylic resin is completed with the PTL-MM01 Dip Coater instrument for obtaining a functionalization layer uniformity. In the subsequent stage, the MEMS sensor is dried for 30 minutes at standard laboratory temperature (25°C) and humidity level (31%) to achieve uniformity in the drying process and achieve the sensor functional stability. The effects of interfering parameters associated with the functionalization process, including time, speed and their effect on the thickness of the functionalization, are examined in the presented study. Also, a MEMS sensor having a varying functionalization thickness is prepared for finding out the influence of the thickness of the functionalization layer on the sensitivity and the output of the MEMS sensor. The increasing functionalization thickness is achieved by changing the speed of withdrawal and time of dipping.

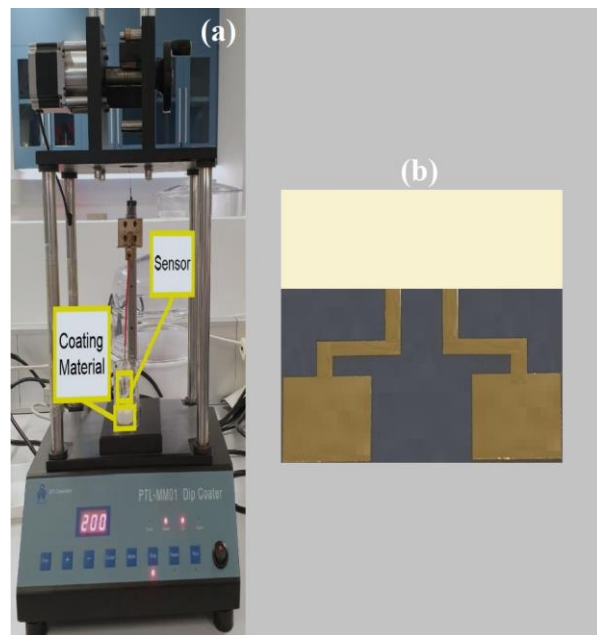


Fig. 3. (a) MIP functionalization process using PTL-MM01 Dip Coater instrument and (b) MIP coated MEMS sensor.

C. Specifically Selective Functionalization Material for Creatinine on the MEMS Sensing Area

As the acrylic resin-coated sensor is not strictly selective against the target biomolecule, e.g. creatinine, the coated MEMS sensing surface cannot specifically and selectively analyse creatinine levels from the serum samples. It is due to the presence of various other biomolecules inside the serum samples. To avoid this issue, the sensing surface of the MEMS sensor is selectively functionalized with a specifically selective synthetic functionalization material. A chemically synthesised MIP methodology is introduced while synthesising a creatinine specific selective functionalization material. MIP is a robust and convenient methodology to synthesise synthetic-detection sites for the target molecule [38] - [39]. MIP is synthesised with the help of the precipitation polymerisation methodology described in our earlier publication [18].

MAA is used as a functional monomer (0.510 mL), AIBN as a reaction initiator (3.22 mL) and divinylbenzene as a cross-linker (7.50 mL). Creatinine is used as a template molecule (0.10 grams of creatinine powder into 2 mL of Milli-Q water in an Eppendorf tube). By mixing the template molecule, a functional monomer, and a cross-linker molecule at a ratio of 2:0.510:7.5, a solvent mixture is made in a flask. To that flask, acetonitrile (96 mL) and toluene (32 mL) are added in 3:1 proportion, and a MIP reaction mixture is prepared. The addition of the reaction initiator to the reaction mixture is then performed, followed by keeping the flask inside a 60°C water bath for initialisation of the process of polymerisation. The complete polymerisation took 24 hrs time frame. In the subsequent stage, the extraction of the template molecule from the core of the MIP polymer is successfully performed with 24 hrs of acetic acid reflux process using a soxhlet extraction apparatus. The use of soxhlet extraction techniques aid in leaving MIP detection sites vacant, and the empty polymer is

obtained having complementary sites for the target molecule, i.e. creatinine. The MIP synthesis associated conditions have been optimised. The corresponding results are provided in our previous article [18].

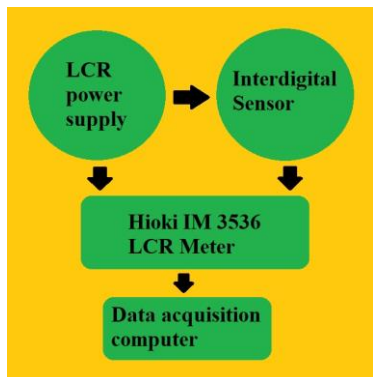


Fig. 4. Diagrammatic representation of the complete EIS measurement system.

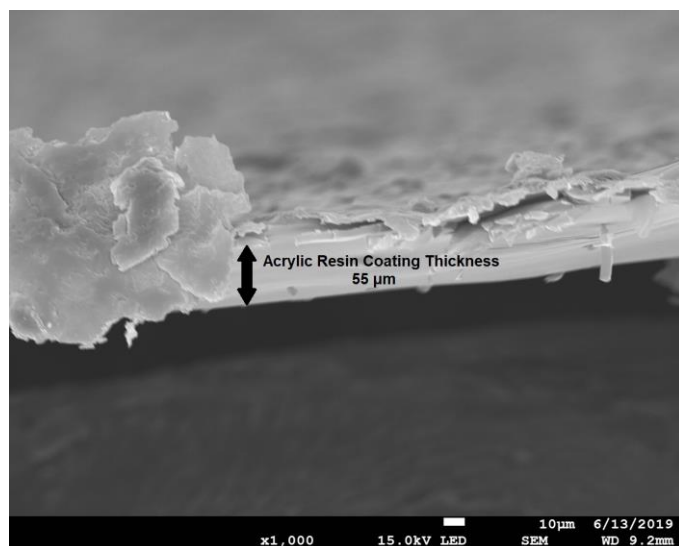


Fig. 5. FESEM images of the acrylic resin coated layer.

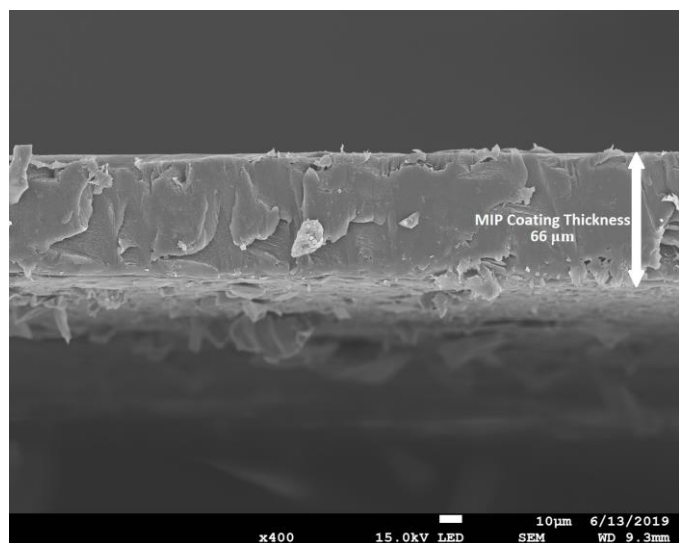


Fig. 6. FESEM images of the selective MIP-polymer coated layer [18].

In the first step, the MEMS sensor is surface cleaned using acetone for removing all kinds of surface impurities. In the subsequent stage, a MIP functionalization material suspension is made by uniformly mixing acetone as a liquefier (1.5 mL), MIP as a selective polymer (1 g), and acrylic resin (200 μ L) as a protective layer of the functionalization as well as adhesive agent in a small beaker at laboratory temperature.

The saturation of thickness of the functionalization layer is dependent on functionalization material properties and the dip coating process (speed of withdrawal and dipping time). To avoid rapid evaporation of acetone at laboratory temperature, drying out of both acrylic functionalization solution and the MIP suspension functionalization solution, instant cracking/peeling off of the functionalization layers from the MEMS ID sensing area, the following essential factors need to be taken into consideration. The liquid suspension bottles containing acrylic and MIP functionalization solutions should be strictly stored inside the freezer at -4°C and taken out only for 15-20 minutes before the process of functionalization. It helps in slowly increasing the temperature of bottles to laboratory temperature. The lid of the glass storage bottles should be opened only for the time of the dip coating procedure. It should be closed right after finishing the dipping experiment, followed by restoring the solutions at a -4°C freezer. To avoid rapid evaporation of acetone and consecutive instant cracking of both acrylic functionalization solution and the MIP functionalization layer suspension, the individual solution temperatures are maintained at laboratory temperature and humidity level. The effect of thickness and consistency of both acrylic functionalization solution and the MIP functionalization solutions are studied in our earlier published article [18]. A PTL-MM01 Dip Coater instrument is used in the process of functionalization, as shown in Fig. 3 (a).

Post functionalization, the sensor is slowly and uniformly withdrawn from the functionalization suspension solutions to achieve uniformity in both the acrylic functionalization and the MIP polymer selective functionalization layers. Both the coated MEMS sensors are air-dried for 1 hr at average laboratory temperature in the final stage. The increasing functionalization thickness is achieved by changing the speed of withdrawal and time of dipping. Fig. 3 (b) displays the functionalized MEMS sensor with a MIP polymer functionalization. The creatinine binding procedure on MIP coated MEMS sensor is studied [18], [23], [24], and experiments are done with the EIS technique using the LCR meter instrument. Streptavidin is also used in literature for the biosensor functionalization process. However, in our application, the acrylic resin acted as the optimum functionalization agent. It created a protective layer of the functionalization and worked as an excellent adhesive agent.

D. Experimentation Set-up and the Apparatus

Series of experiments are carried out with the help of high precision Hioki 3536 LCR meter instrument. The instrument is adjusted on a slow mode of operation for significantly rising the precision of obtained results. To ensure the results reliability, the readings are repeated 5 times, and an average of 5 readings is considered. With the aid of gold pin connectors, the MEMS sensor is connected to the Hioki 3536 LCR meter,

and the Hioki 3536 is used to record the parameters. The LCR meter is further linked to the data acquisition system. Fig. 4 shows the process diagram of the full EIS analysis measuring scheme. The sensing area of the MEMS sensor is coated with the help of the PTL-MM01 Dip Coater instrument to achieve the sensor functionalization for selective detection and capturing of creatinine molecule from the samples. The FESEM instrument is used for obtaining high-definition images of the MEMS sensor functionalized surfaces. The FESEM images of the acrylic resin coated layer, and the MIP-polymer coated selective layer are displayed in Fig. 5 as well as Fig. 6.

IV. RESULTS AND DISCUSSIONS

A. Creatinine Level Analysis with the Acrylic Resin & MIP Coated MEMS ID Sensor

A stock solution of 100 ppm is made by dissolving 1-mg of creatinine powder in 10 mL of heat-inactivated human serum stored inside the refrigerator. A technique of serial dilution is used for preparing samples with varying concentration levels (6 ppm, 10 ppm, 14 ppm and 15 ppm).

The normal creatinine range in human serum for females is 0.5–1.1 mg/dL (5–11 ppm), whereas, for men, it is 0.6–1.2 mg/dL (6–12 ppm). It is due to the gender-specific body composition having slightly higher levels of skeletal lean muscle mass. Serum creatinine levels over 15 ppm need medical attention. For creatinine selective detection, the MIP coated MEMS ID sensors detection limit is 50 ppm, which is three times higher than the expected level of creatinine concentration in human serum [18]. The ability of the MIP coated MEMS ID sensor to detect up to 50 ppm is useful in case if the coated sensor is used for serum sample having very high creatinine levels.

In the initial step, the creatinine measurement is done using an acrylic resin coated MEMS sensor prepared with varying thickness of the functionalization's (55, 120, 180, 240 μm). The MEMS sensor gets saturated at 240 μm thickness of the acrylic resin functionalization. Varying thicknesses of functionalization layers are attained by repeating the functionalization process.

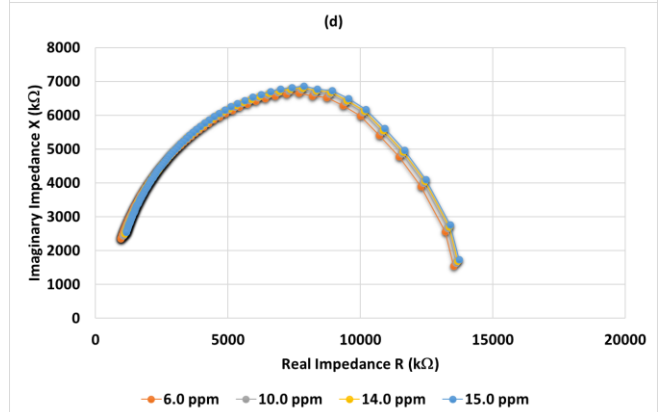
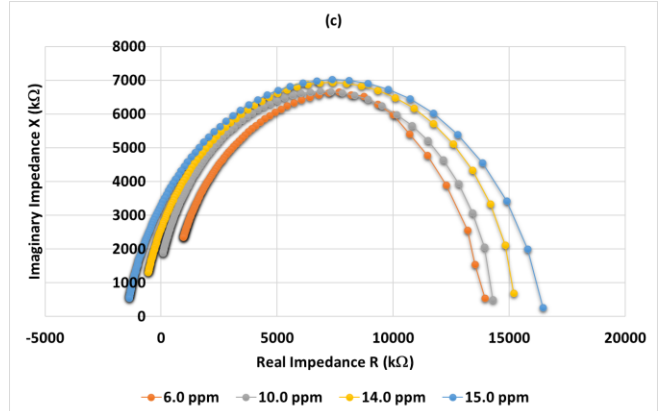
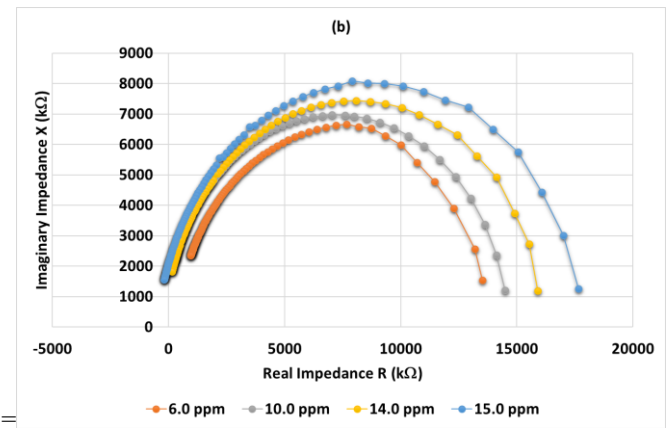
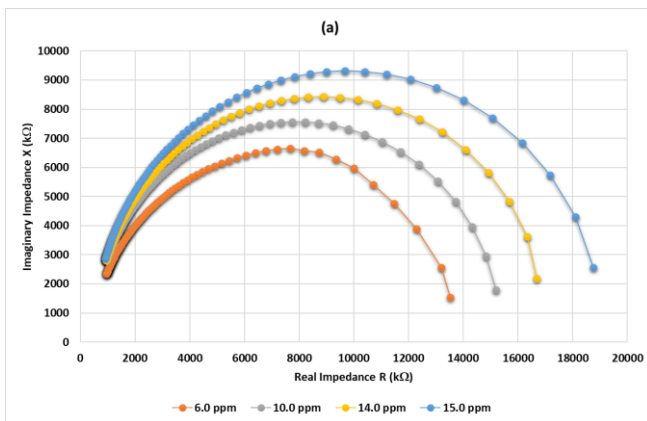
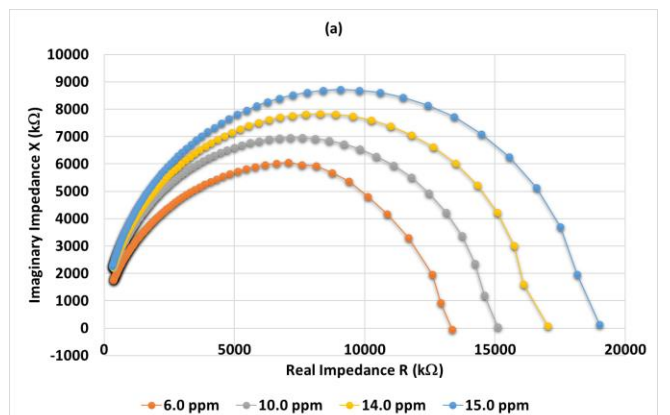


Fig. 7. Serum creatinine analysis with the help of acrylic-coated MEMS sensor having a varying thickness of coats: (a) 55 μm , (b) 120 μm , (c) 180 μm , (d) 240 μm .



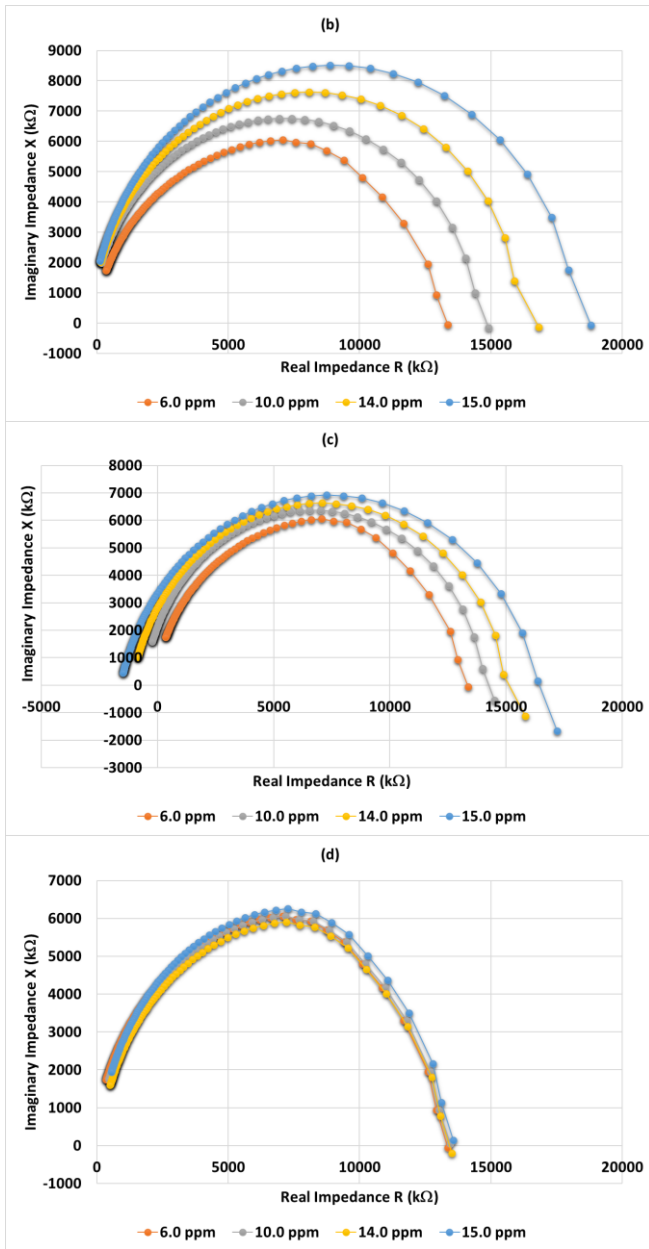


Fig. 8. Serum creatinine analysis with the help of MIP-coated MEMS sensor having a varying thickness of coats: (a) 66 μm , (b) 135 μm , (c) 200 μm , (d) 270 μm .

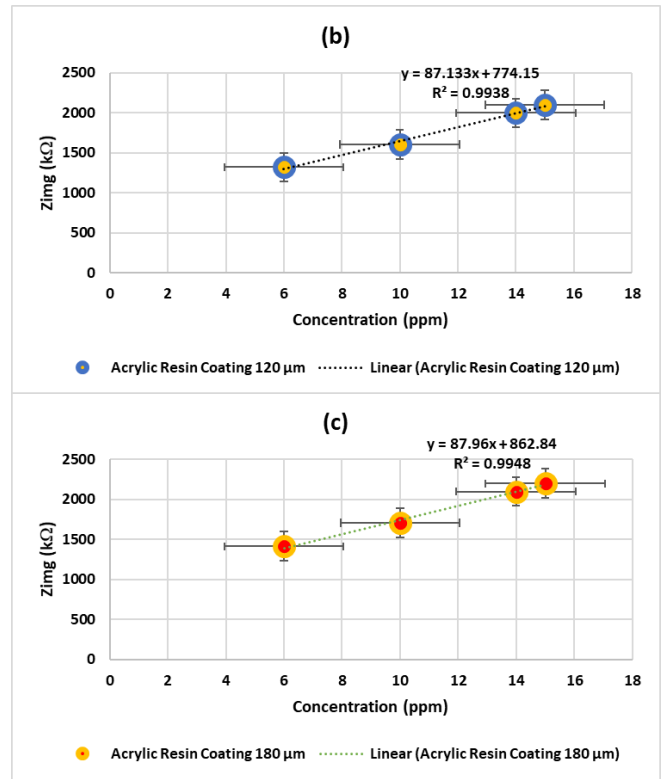
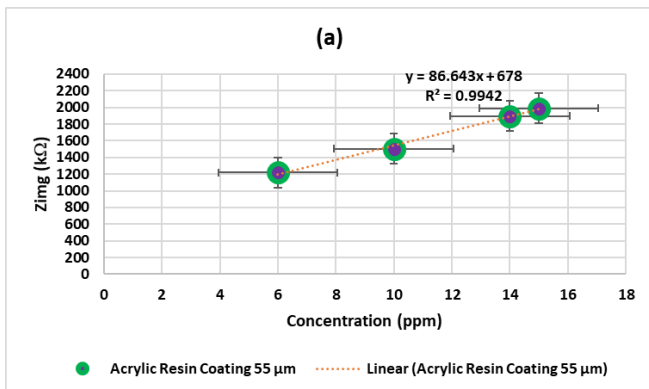
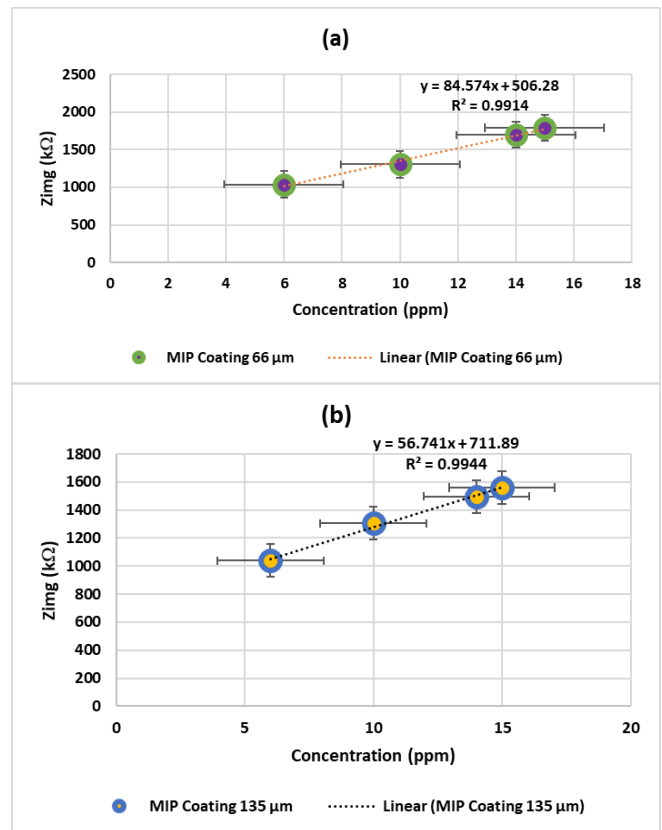


Fig. 9. Acrylic resin-coated sensors calibration curves for the varying thickness of functionalization's: (a) 55 μm , (b) 120 μm , (c) 180 μm .



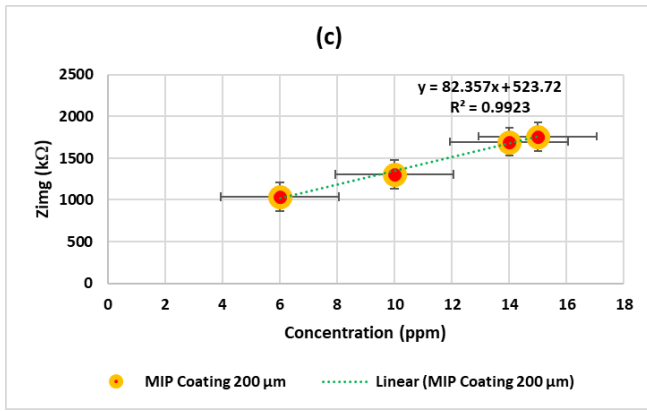


Fig. 10. MIP coated sensors calibration curves for the varying thickness of functionalization's: (a) 66 μm , (b) 135 μm , (c) 200 μm .

Post functionalization of the MEMS sensor with acrylic resin, profiling of the coated sensor has been done in the air. It is tested with the serum samples solutions of varying creatinine levels. The same set of experiments are performed with the 55, 120, 180, 240 μm . Fig. 7 denotes experimental results in the representation style of the Nyquist plotting technique.

It is noticed that the bidirectional changes happened for the real as well as the imaginary impedance for thickness levels ranging from 55 μm to 240 μm . It is observed that as functionalization layer thickness decreases, the differences displayed within every Nyquist plot for various creatinine concentrations are significantly distinct. Nevertheless, the acrylic resin coated MEMS sensor having 240 μm thickness of functionalization did not show significant changes in varying creatinine concentrations.

In the initial step of MIP-coated MEMS sensor creatinine concentration analysis, the uncoated MEMS sensor is characterised using the EIS technique with an LCR meter to determine the sensitive frequency range used MEMS sensor. The MIP functionalization process is done, and thickness levels of MIP polymer functionalization's (66, 135, 200, 270 μm) is achieved. Post functionalization process, the MEMS sensor with MIP is re-characterised in the air for comparing the profiles of varying MIP functionalization thicknesses. It is noticed that the size of the diameter of the semicircle of the Nyquist plot changes with varying thicknesses. It is also observed that the Nyquist plot semicircle comparatively gets saturated at 270 μm when coated using MIP. It is because of a heavier functionalization thickness level over the penetration capacity of the protruding electrical field.

In the next set of experiments, the MIP polymer coated MEMS sensor is utilised for testing the creatinine serum samples. Varying thickness levels of MIP polymer functionalization's (66, 135, 200, 270 μm) are achieved using the PTL-MM01 Dip Coater instrument by performing a repetitive dipping technique. The same procedure is used whilst performing experiments with the help of the MIP coated MEMS sensor. Four samples having varying creatinine concentrations are analysed by using MIP coated MEMS sensor. The Nyquist plot for the MEMS sensor coated with MIP polymer having varying functionalization thickness (66, 135, 200, 270 μm) is displayed in Fig. 8. Concerning MIP

functionalization thickness levels ranging from 66 μm to 270 μm , a rise in the Nyquist plot semicircular region diameter indicates a clear rise in creatinine concentrations in serum samples. The increase in the Nyquist plot diameter is due to the rise in the number of creatinine molecules [18], [23].

Nonetheless, it is found that the MEMS sensor is saturated at 270 μm and did not display significant changes in the varying amounts of creatinine. The MIP polymer is selectively synthesised for adsorbing the creatinine molecules from the sample solution [18], [23], [24]. Therefore, the MIP coated MEMS ID sensor showed much better performance than the acrylic-coated one.

The two different functionalization materials (acrylic and MIP) are saturated at two different thicknesses. The acrylic functionalization solution is made by mixing acetone as a liquefier and acrylic resin. The MIP functionalization suspension is composed of acetone as a liquefier, MIP as a selective polymer, acrylic resin as a protective layer of the functionalization and an adhesive agent. The acetone gets evaporated, but the combination of MIP and acrylic resin shows an effect on the thickness of the MIP suspension functionalization, making it thicker after drying the coat. Although the MIP suspension functionalization has shown higher thickness (66, 135, 200, 270 μm) for all the functionalization's over acrylic functionalization solution (55, 120, 180, 240 μm), it is found to be displaying the higher sensitivity. It is due to the usage of creatinine (template molecule), MAA (functional monomer), AIBN (reaction initiator), and divinylbenzene (cross-linker) in the synthesis of MIP. Their cross-linking made the MIP polymer highly selective, sensitive, and specific towards adsorption of the creatinine from the spiked serum creatinine samples.

B. Coated MEMS Sensor Sensitivity and the Saturation Level Measurement

A coated sensor with varying thicknesses of the functionalization is used to obtain the calibration curve derived from investigating the MEMS sensor output-related sensitivity. By plotting the imaginary impedance against creatinine concentration at 1020 Hz (operating frequency), the calibration curves are derived. As maximum changes are noticed with the imaginary impedance at 1020 Hz, it is chosen over the real impedance [18], [23]. The acrylic resin coated MEMS sensor calibration curves with three varying functionalization thicknesses are shown in Fig. 9. Fig. 10 shows the MIP coated MEMS sensor having three varying functionalization thicknesses calibration curves.

By using the slope of the calibration curves, the MEMS sensor sensitivity is indicated. It is found that with the increase in functionalization layer thickness, the curve slope gets affected. This phenomenon occurs because of the passing of the fewer electric lines from the sample when the MEMS functionalization thickness level is increased. It is also noticed that for achieving the highest sensitivity, the thinnest functionalization layer is most useful. Fig. 11 displays both functionalization's sensitivity (acrylic resin coated and MIP-coated) at varying functionalization thicknesses. As described in Fig. 11, the MIP-coated MEMS ID biosensors sensitivity is 0.15 Ω/ppm .

It is noticed that in both the functionalization's, a linear decrease in sensitivity is found. It is linked with a rise in the thickness of the functionalization. The MIP coated MEMS sensor displayed higher sensitivity and selectivity towards capturing creatinine from serum samples over the acrylic resin coated MEMS sensor. The MIP is specifically synthesised by using creatinine molecule as a template. Therefore, the MIP suspension solution functionalization on the MEMS sensor displayed higher sensitivity [18], [23], [24].

Serum creatinine samples with different creatinine levels have been analysed with coated sensors to verify the MEMS sensor saturation level, and the results are shown in Fig. 12. A direct relation is observed between the increase of the functionalization layer thickness and the enhancement in the level of saturation. This is related to the availability of more creatinine specific capturing sites and to the increasing thickness of the functionalization. Nevertheless, it also reaches the saturation level when the MEMS sensor sensing surface is dense with capturing sites. However, the increasing thickness of the functionalization also hampers the passing of the electric field. Thus, a compromise is chosen for the sensitivity and saturation level after finalising the functionalization thickness.

C. Thickness of Functionalization Reliance on the Speed of Withdrawal and Time of Dipping

When the PTL-MM01 Dip Coater instrument is utilised for the process of dipping, the functionalization layer thickness is analysed by studying the speed of withdrawal and time of dipping for the MEMS sensor. The acrylic functionalization solution and the MIP suspension solution are used to conduct this analysis.

The dipping time is pre-set for 10 seconds, and the withdrawal speed is changed from 50 mm/s (minimum speed available) to 200 mm/s (maximum speed available). It is done to investigate the effect of the withdrawal speed on the functionalization thickness. The reliance of the functionalization thickness on the withdrawal speed is seen (Fig. 13). The functionalization layer thickness is raised from 55 μm to 240 μm for the acrylic resin functionalization suspension.

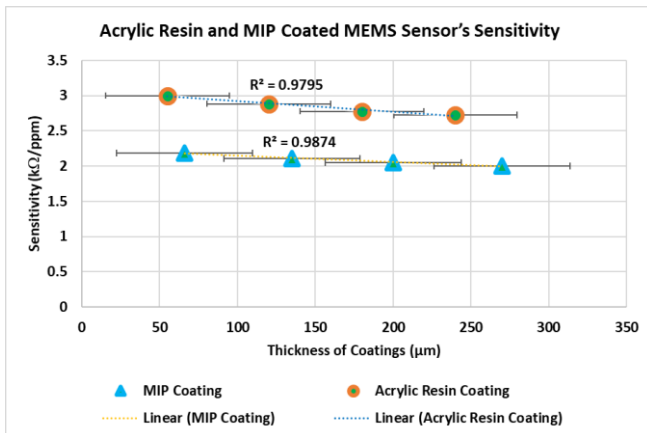


Fig. 11. The acrylic resin and MIP coated MEMS sensor sensitivity.

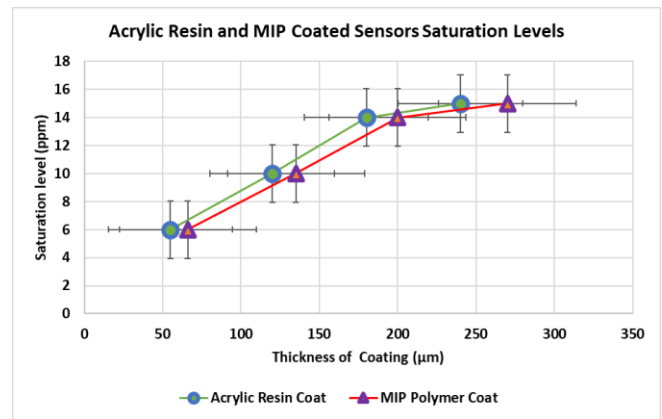


Fig. 12. Acrylic resin and MIP coated sensors saturation levels.

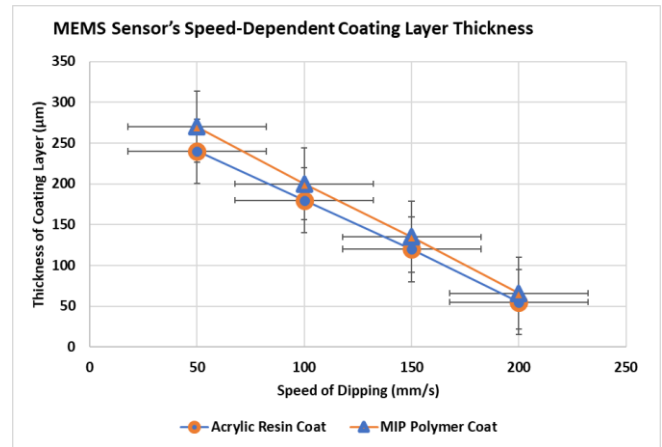


Fig. 13. MEMS sensor speed of withdrawal-dependent functionalization layer thickness.

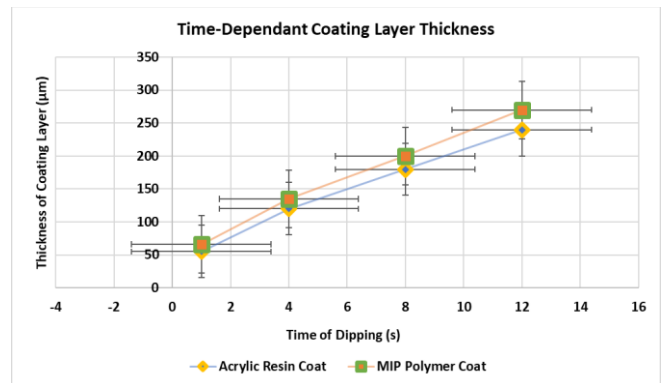


Fig. 14. A time-dependant functionalization layer thickness.

For MIP functionalization material functionalization suspension, the functionalization layer thickness is raised from 66 μm to 270 μm . The maximum thickness is observed at 50 mm/s withdrawal speed.

For identifying the time-dependent functionalization thickness, the speed of withdrawal is maintained at 200 mm/s, and the time of dipping inside the functionalization suspension solution is altered from 1 second to 12 seconds. Fig. 14 shows the outcome of the functionalization layer thickness concerned with the time of dipping. It is detected that the sufficient thickness of the functionalization layer is obtained in 1

second. In contrast, the highest level of thickness is obtained in 12 seconds for acrylic resin and the MIP functionalization material suspension solutions.

V. Conclusion

In the presented work, a planar ID MEMS sensor is effectively coated using acrylic resin and MIP suspension solution. The experiments are done for studying the functional and performance sensitivity of the MEMS sensor in creatinine serum solution. The serum solutions are made using four varying creatinine concentrations, ranging from 6, 10, 14 and 15 ppm. The results showed that acrylic resin and MIP suspension solution show sensitivity towards the creatinine molecules. However, the MIP suspension solution functionalization on the MEMS sensor displayed higher sensitivity. The serum creatinine samples selectivity is related to the acrylic resin-MIP coated MEMS sensor in the capturing process. It is due to the presence of creatinine specific capturing sites inside the MIP functionalization suspension solution. It is also noticed that both the type of functionalization's applied to the MEMS sensor exhibited lesser sensitivity with an increase in the thickness of the functionalization layer on the MEMS sensor. It is also seen that increase in functionalization layer thickness raises the saturation level. Therefore, to find a balance between the amounts of SUT concentrations and the sensitivity, the functionalization thickness must be pre-decided according to the application requirement.

In the presented work, the PTL-MM01 Dip Coater instrument is used to process dip coating to generate a uniform functionalization layer on the MEMS sensing surface. While performing the dip coating process, the functionalization thickness relies on the functionalization material properties, speed of withdrawal and time of dipping. In conclusion, the functionalization thickness is increased by decreasing the speed of withdrawal and increasing the time of immersion. Functionalization layer thinness could be attained with the dip coating technique. For the acrylic resin, it is 55 μm , and for the MIP functionalization solution, the material functionalization thinness is 66 μm .

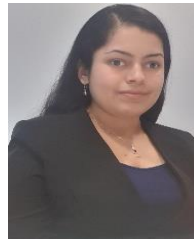
ACKNOWLEDGMENT

The authors are thankful to Macquarie University, NSW, Australia, for providing the experimental facilities. They would also like to convey their sincere thanks to Macquarie University Microscopy Unit Facility, Faculty of Science and Engineering for providing excellent assistance in providing the FESEM images.

REFERENCES

- [1] T. Coan, G. S. Barroso, G. Motz, A. Bolzán, R. A. F. Machado, "Preparation of PMMA/hBN composite coatings for metal surface protection," *Mater. Res.*, vol. 16, no. 6, pp. 1366 – 1372, 2013, doi: [10.1590/S1516-14392013005000140](https://doi.org/10.1590/S1516-14392013005000140).
- [2] H. -C. Wang, A. Zyuzin, A. V. Mamishev, "Measurement of coating thickness and loading using concentric fringing electric field sensors," *IEEE Sensors J.*, vol. 14, no. 1, pp. 68 – 78, Jan. 2014, doi: [10.1109/JSEN.2013.2279991](https://doi.org/10.1109/JSEN.2013.2279991).
- [3] A. Azmi et al., "Performance of coating materials on planar electromagnetic sensing array to detect water contamination," *IEEE Sensors J.*, vol. 17, no. 16, pp. 5244 – 5251, Aug. 2017, doi: [10.1109/JSEN.2017.2720701](https://doi.org/10.1109/JSEN.2017.2720701).
- [4] J. H. Snoeijer, J. Ziegler, B. Andreotti, M. Fermigier, J. Eggers, "Thick films of viscous fluid coating a plate withdrawn from a liquid reservoir," *Phys. Rev. Lett.*, vol. 100, p. 244502, Jun. 2008, doi: [10.1103/PhysRevLett.100.244502](https://doi.org/10.1103/PhysRevLett.100.244502).
- [5] S. Krishnan, C. J. Weinman, C. K. Ober, "Advances in polymers for anti-biofouling surfaces," *J. Mater. Chem.*, vol. 18, no. 29, pp. 3405 – 3413, 2008, doi: [10.1039/B801491D](https://doi.org/10.1039/B801491D).
- [6] A. E. Nel et al., "Understanding biophysicochemical interactions at the nano-bio interface," *Nature Mater.*, vol. 8, pp. 543 – 557, Jun. 2009, doi: [10.1038/nmat2442](https://doi.org/10.1038/nmat2442).
- [7] S. Viswanathan, C. Rani, S. Ribeiro, C. Delerue-Matos, "Molecular imprinted nanoelectrodes for ultra-sensitive detection of ovarian cancer marker," *Biosensors Bioelectron.*, vol. 33, pp. 179 – 183, Mar. 2012, doi: [10.1016/j.bios.2011.12.049](https://doi.org/10.1016/j.bios.2011.12.049).
- [8] A. I. Zia, S. C. Mukhopadhyay, P. -L. Yu, I. H. Al-Bahadly, C. P. Gooneratne, J. Kosel, "Rapid and molecular selective electrochemical sensing of phthalates in aqueous solution," *Biosensors Bioelectron.*, vol. 67, pp. 342 – 349, May 2015, doi: [10.1016/j.bios.2014.08.050](https://doi.org/10.1016/j.bios.2014.08.050).
- [9] A. Aghaei, M. R. M. Hosseini, M. Najafi, "A novel capacitive biosensor for cholesterol assay that uses an electropolymerised molecularly imprinted polymer," *Electrochim. Acta*, vol. 55, pp. 1503 – 1508, Feb. 2010, doi: [10.1016/j.electacta.2009.09.033](https://doi.org/10.1016/j.electacta.2009.09.033).
- [10] M. Nebi, D. Peker, "Effect of heat treatment on the structural properties of TiO₂ films produced by sol-gel spin coating technique," *J. Phys., Conf. Ser.*, vol. 766, no. 1, p. 012026, 2016, doi: [10.1088/1742-6596/766/1/012026](https://doi.org/10.1088/1742-6596/766/1/012026).
- [11] S. Ilcan, "Structural, optical and electrical properties of erbium-doped ZnO thin films prepared by spin coating method," *J. Nanoelectron. Optoelectron.*, vol. 11, pp. 465 – 471, Aug. 2016, doi: [10.1166/jno.2016.1934](https://doi.org/10.1166/jno.2016.1934).
- [12] M. Wong et al., "Large-scale self-assembled zirconium phosphate smectic layers via a simple spray-coating process," *Nature Commun.*, vol. 5, p. 3589, Apr. 2014, doi: [10.1038/ncomms4589](https://doi.org/10.1038/ncomms4589).
- [13] Y. Guo, W. Li, H. Yu, D. F. Perepichka, H. Meng, "Flexible asymmetric supercapacitors via spray coating of a new electrochromic donor-acceptor polymer," *Adv. Energy Mater.*, vol. 7, no. 2, pp. 1 – 7, 2017, doi: [10.1002/aenm.201601623](https://doi.org/10.1002/aenm.201601623).
- [14] D. Grosso, "How to exploit the full potential of the dip coating process to better control film formation," *J. Mater. Chem.*, vol. 21, pp. 17033 – 17038, Oct. 2011, doi: [10.1039/C1JM12837J](https://doi.org/10.1039/C1JM12837J).
- [15] S. H. Chaki, M. Deshpande, J. P. Taylor, "Characterisation of CuS nanocrystalline thin films synthesised by chemical bath deposition and dip coating techniques," *Thin Solid Films*, vol. 550, pp. 291 – 297, Jan. 2014, doi: [10.1016/j.tsf.2013.11.037](https://doi.org/10.1016/j.tsf.2013.11.037).
- [16] R. Ashiri, A. Nemati, M. S. Ghamsari, "Crack-free nanostructured BaTiO₃ thin films prepared by sol-gel dip coating technique," *Ceram. Int.*, vol. 40, pp. 8613 – 8619, Jul. 2014, doi: [10.1016/j.ceramint.2014.01.078](https://doi.org/10.1016/j.ceramint.2014.01.078).
- [17] X. Zhang, H. Ye, B. Xiao, L. Yan, H. Lv, B. Jiang, "Sol-Gel preparation of PDMS/silica hybrid antireflective coatings with controlled thickness and durable antireflective performance," *J. Phys. Chem. C*, vol. 114, pp. 19979 – 19983, Nov. 2010, doi: [10.1021/jp106192z](https://doi.org/10.1021/jp106192z).
- [18] S. N. Prabhu, S. C. Mukhopadhyay, C. P. Gooneratne, A. S. Davidson, G. Liu, "Molecularly Imprinted Polymer-based detection of creatinine towards smart sensing," *Medical Devices and Sensors*, 2020, doi: [10.1002/mds3.10133](https://doi.org/10.1002/mds3.10133).
- [19] S. N. Prabhu, S. C. Mukhopadhyay, A. S. Davidson and G. Liu, "Highly selective Molecularly Imprinted Polymer for creatinine detection," 2019 13th International Conference on Sensing Technology (ICST), 2019, pp. 1-5, doi: [10.1109/ICST46873.2019.9047696](https://doi.org/10.1109/ICST46873.2019.9047696).
- [20] S. N. Prabhu, S. C. Mukhopadhyay, C. Gooneratne, A. S. Davidson and G. Liu, "Interdigital sensing system for detection of levels of creatinine from the samples," 2019 13th International Conference on Sensing Technology (ICST), 2019, pp. 1-6, doi: [10.1109/ICST46873.2019.9047672](https://doi.org/10.1109/ICST46873.2019.9047672).

- [21] S. Prabhu, C. Gooneratne, K. Anh Hoang and S. Mukhopadhyay, "Development of a Point-of-Care diagnostic smart sensing system to detect creatinine levels," 2020 IEEE 63rd International Midwest Symposium on Circuits and Systems (MWSCAS), 2020, pp. 77-80, doi: [10.1109/MWSCAS48704.2020.9184441](https://doi.org/10.1109/MWSCAS48704.2020.9184441).
- [22] C. Miura, N. Funaya, H. Matsunaga, J. Haginaka, "Monodisperse, molecularly imprinted polymers for creatinine by modified precipitation polymerisation and their applications to creatinine assays for human serum and urine," Journal of Pharmaceutical and Biomedical Analysis, vol. 85, pp. 288 – 294, 2013, doi: [10.1016/j.jpba.2013.07.038](https://doi.org/10.1016/j.jpba.2013.07.038).
- [23] S. Prabhu, C. Gooneratne, K. A. Hoang and S. Mukhopadhyay, "IoT-Associated Impedimetric Biosensing for Point-of-Care Monitoring of Kidney Health," in IEEE Sensors Journal, doi: [10.1109/JSEN.2020.3011848](https://doi.org/10.1109/JSEN.2020.3011848).
- [24] Prabhu S.N., Gooneratne C.P., Hoang K.A., Mukhopadhyay S.C., Davidson A.S., Liu G. (2021) Interdigital Sensing System for Kidney Health Monitoring. In: Mukhopadhyay S.C., George B., Roy J.K., Islam T. (eds) Interdigital Sensors. Smart Sensors, Measurement and Instrumentation, vol 36. Springer, Cham, doi: [10.1007/978-3-030-62684-6_11](https://doi.org/10.1007/978-3-030-62684-6_11).
- [25] A. V. Mamishev, K. Sundara-Rajan, F. Yang, Y. Du, M. Zahn, "Interdigital sensors and transducers," Proc. IEEE, vol. 92, no. 5, pp. 808 – 845, May 2004, doi: [10.1109/JPROC.2004.826603](https://doi.org/10.1109/JPROC.2004.826603).
- [26] A. M. Syaifudin et al., "Measurements and performance evaluation of novel interdigital sensors for different chemicals related to food poisoning," IEEE Sensors J., vol. 11, no. 11, pp. 2957 – 2965, Nov. 2011, doi: [10.1109/JSEN.2011.2154327](https://doi.org/10.1109/JSEN.2011.2154327).
- [27] A. M. Syaifudin, S. Mukhopadhyay, P. Yu, "Electromagnetic field computation using COMSOL multiphysics to evaluate the performance of novel interdigital sensors," Proc. Appl. Electromagn. Conf. (AEMC), pp. 1 – 4. Dec. 2009, doi: [10.1109/AEMC.2009.5430661](https://doi.org/10.1109/AEMC.2009.5430661).
- [28] A. I. Zia et al., "Electrochemical impedance spectroscopy based MEMS sensors for phthalates detection in water and juices," J. Phys., Conf. Ser., vol. 439, no. 1, p. 012026, 2013, doi: [10.1088/1742-6596/439/1/012026](https://doi.org/10.1088/1742-6596/439/1/012026).
- [29] M. S. A. Rahman, S. C. Mukhopadhyay, P. -L. Yu, "Novel Sensors for Food Inspection: Modelling, Fabrication and Experimentation," Cham, Switzerland: Springer, 2014, doi: [10.1007/978-3-319-04274-9](https://doi.org/10.1007/978-3-319-04274-9).
- [30] E. J. Olson, P. Bühlmann, "Minimising hazardous waste in the undergraduate analytical laboratory, A microcell for electrochemistry," J. Chem. Edu., vol. 87, no. 11, pp. 1260 – 1261, 2010, doi: [10.1021/ed100495k](https://doi.org/10.1021/ed100495k).
- [31] U. Retter, H. Lohse, "Electrochemical impedance spectroscopy," Electroanalytical Methods. Berlin, Germany: Springer, 2010, pp. 159 – 177, doi: [10.1007/978-3-642-02915-8](https://doi.org/10.1007/978-3-642-02915-8).
- [32] N. Afsarimanesh et al., "Smart sensing system for the prognostic monitoring of bone health," Sensors, vol. 16, p. 976, Jan. 2016, doi: [10.3390/s16070976](https://doi.org/10.3390/s16070976).
- [33] N. Afsarimanesh, S. C. Mukhopadhyay, M. Kruger, "Molecularly imprinted polymer-based electrochemical biosensor for bone loss detection," IEEE Trans. Biomed. Eng., vol. 65, no. 6, pp. 1264 – 1271, 2018, doi: [10.1109/TBME.2017.2744667](https://doi.org/10.1109/TBME.2017.2744667).
- [34] M. S. A. Rahman et al., "Detection of bacterial endotoxin in food: New planar interdigital sensors based approach," J. Food Eng., vol. 114, pp. 346 – 360, Feb. 2013, doi: [10.1016/j.jfoodeng.2012.08.026](https://doi.org/10.1016/j.jfoodeng.2012.08.026).
- [35] A. I. Zia, S. C. Mukhopadhyay, P.-L. Yu, I. H. Al-Bahady, C. P. Gooneratne, J. Kosel, "Rapid and molecular selective electrochemical sensing of phthalates in aqueous solution," Biosensors Bioelectron., vol. 67, pp. 342 – 349, May 2015, doi: [10.1016/j.bios.2014.08.050](https://doi.org/10.1016/j.bios.2014.08.050).
- [36] S. N. Prabhu, C. P. Gooneratne and S. C. Mukhopadhyay, "Development of MEMS Sensor for Detection of Creatinine using MIP Based Approach -A Tutorial Paper," in IEEE Sensors Journal, doi: [10.1109/JSEN.2021.3077060](https://doi.org/10.1109/JSEN.2021.3077060) (early access).
- [37] C. Alexander et al., "Molecular imprinting science and technology: A survey of the literature for the years up to and including 2003," J. molecular Recognit., vol. 19, no. 2, pp. 106 – 180, 2006, doi: [10.1002/jmr.760](https://doi.org/10.1002/jmr.760).
- [38] A. Bossi, F. Bonini, A. P. F. Turner, S. A. Piletsky, "Molecularly imprinted polymers for the recognition of proteins: The state of the art," Biosensors Bioelectron., vol. 22, pp. 1131 – 1137, Jan. 2007, doi: [10.1016/j.bios.2006.06.023](https://doi.org/10.1016/j.bios.2006.06.023).
- [39] G. Díaz-Díaz, D. Antuña-Jiménez, M. C. Blanco-López, M. J. Lobo-Castañón, A. J. Miranda-Ordieres, P. Tuñón-Blanco, "New materials for analytical biomimetic assays based on affinity and catalytic receptors prepared by molecular imprinting," TrAC Trends Anal. Chem., vol. 33, pp. 68 – 80, Mar. 2012, doi: [10.1016/j.trac.2011.09.011](https://doi.org/10.1016/j.trac.2011.09.011).



Ms Sumedha N. Prabhu received the B.Sc. degree in Biotechnology from the University of Mumbai, India, in 2011, and the master's degree in Biotechnology from the University of Mumbai, India, in 2013.

She is currently pursuing a PhD degree in sensors and smart sensing system from the School of Engineering, Faculty of Science and Engineering, Macquarie University, Sydney, Australia. Her research interest includes smart sensing systems, the Internet of Things (IoT), and embedded systems for

the early detection of various diseases in humans. Sumedha is awarded AUD 5000.00, a highly competitive Macquarie University Postgraduate Research Fund grant during her early third year of PhD. Sumedha has received two People's Choice Awards during her PhD candidature. More details can be available at <https://researchers.mq.edu.au/en/persons/sumedha-prabhu>



Prof. Subhas C. Mukhopadhyay (M'97, SM'02, F'11) holds a B.E.E. (gold medallist), M.E.E., PhD (India) and Doctor of Engineering (Japan). He has over 31 years of teaching, industrial and research experience.

Currently, he is working as a Professor of Mechanical/Electronics Engineering, Macquarie University, Australia, and is the Discipline Leader of the Mechatronics Engineering Degree Programme. He is also the Director of International Engagement for the School of Engineering of Macquarie

University. His fields of interest include Smart Sensors and sensing technology, instrumentation techniques, wireless sensors and network (WSN), Internet of Things (IoT), wearable sensors and medical devices. He has supervised over 40 postgraduate students and over 100 Honours students. He has examined over 60 postgraduate theses.

He has published over 400 papers in different international journals and conference proceedings, written nine books and forty-two book chapters and edited eighteen conference proceedings. He has also edited thirty-five books with Springer-Verlag and thirty journal special issues. He has organized over 20 international conferences as either General Chairs/co-chairs or Technical Programme Chair. He has delivered 375 presentations, including keynote, invited, tutorial and special lectures.

He is a **Fellow of IEEE** (USA), a **Fellow of IET** (UK), a **Fellow of IETE** (India), a Topical Editor of IEEE Sensors journal, an associate editor of IEEE Transactions on Instrumentation and Measurements, an Associate Editor of IEEE Systems Journal and IEEE Review of Biomedical Engineering. He is the Editor-in-Chief of the International Journal on Smart Sensing and Intelligent Systems. He is a Distinguished Lecturer of the IEEE Sensors Council from 2017 to 2022. He is the Founding Chair of the IEEE Sensors Council New South Wales Chapter. More details can be available at <https://researchers.mq.edu.au/en/persons/subhas-mukhopadhyay> <https://scholar.google.com.au/citations?hl=en&user=8p-BvWIAAAJ> <https://orcid.org/0000-0002-8600-5907>

Dr Rosario Morello (M'03) is born in Reggio Calabria, Italy, in 1978. He received the M.Sc. Degree (cum laude) in Electronic Engineering and the PhD degree in Electrical and Automation Engineering from the University Mediterranea of Reggio Calabria, Italy, in 2002 and 2006, respectively. Since 2005, he has been a Postdoctoral Researcher of Electrical and Electronic Measurements at the Department of Information Engineering, Infrastructure and Sustainable Energy of the same University.

At present, he is Associate Professor. He is the Scientific Director of the Advanced Thermography Center of the University Mediterranea of Reggio Calabria. His main research interests include the design and characterization of distributed and intelligent measurement systems, wireless sensor network, environmental monitoring, decision-making problems and measurement uncertainty, process quality

assurance, instrumentation reliability and calibration, energy, smart grids, battery testing, biomedical applications and statistical signal processing, noninvasive systems, biotechnologies and measurement, instrumentation and methodologies related to Healthcare. Dr Morello is a member of the Italian Group of Electrical and Electronic Measurements (GMEE).